

# Preparation and tribological properties of graphene oxide/nitrile rubber nanocomposites

Yuqi Li · Qihua Wang · Tingmei Wang ·  
Guangqin Pan

Received: 25 June 2011 / Accepted: 3 August 2011 / Published online: 13 August 2011  
© Springer Science+Business Media, LLC 2011

**Abstract** Graphene oxide (GO)/nitrile rubber (NBR) nanocomposites with various contents of GO were prepared by a solution-mixing method, in this study. The GO sheets were exfoliated from natural fake graphite by an improved Hummers method and could be further dispersed homogeneously in NBR matrix. The thickness and size of the GO sheets were observed by atomic force microscopy and transmission electron microscopy. The tribological properties of the GO/NBR nanocomposites were evaluated on a ring-block MRH-3 wear tester under dry sliding and water-lubricated conditions. The worn surface morphologies of the GO/NBR nanocomposites were observed by a scanning electron microscopy. It was found that under dry sliding, both the friction coefficient (COF) and specific wear rate of the nanocomposites decreased dramatically at first, then increased with increasing GO contents, while under water-lubricated condition, both the COF and specific wear rate of the nanocomposites decreased with increasing GO contents. Finally, the friction and wear mechanisms of the GO/NBR nanocomposites were tentatively proposed.

## Introduction

Graphene has recently enjoyed extensive attention because of its excellent properties, such as high thermal conductivity, high Young's modulus, large specific surface area, electromagnetic interference shielding, and electrical conductivity [1]. These outstanding properties of graphene enable it becomes as bright prospects in various applications for advanced technologies, e.g., solar cells, field-effect devices, practical sensors, transparent electrodes, nanocomposites, etc. [2, 3]. Especially, in the area of polymer nanocomposites, graphene is considered to be one of the most promising modifiers because of its excellent properties, and the pursuit of the research on polymer nanocomposites is towards modifying the neat polymers to attain newer and better properties, without sacrificing their processability or adding excessive weight [4]. Although progresses have been made in the use of graphene sheets as modifiers of polymer matrices, one main factor that limits the application of graphene is the poor compatibility between the pristine graphene sheets and the polymer matrix. In contrast to pristine graphene, there is a plenty of oxygen-containing groups on the GO surface, these functional groups do not only allow the good dispersion of GO in aqueous solution, but also facilitate the interaction between the host polymer and GO via covalent or non-covalent bonds [5]. Thus, it would be more worthwhile to prepare GO/polymer nanocomposites and study their novel properties [6, 7].

In recent years, some study has been reported with respect to the tensile strength, modulus, and the electrical conductivity of GO/polymer nanocomposites. These studies have shown that the nanocomposites exhibited excellent electrical, mechanical, and thermal stability properties [8–12]. In addition, Graphitic carbon has previously been

---

Y. Li · Q. Wang · T. Wang (✉)  
State Key Laboratory of Solid Lubrication, Lanzhou Institute  
of Chemical Physics, Chinese Academy of Sciences,  
Lanzhou 730000, People's Republic of China  
e-mail: wangtin3088@sina.com

Y. Li  
Graduate School of Chinese Academy of Sciences,  
Beijing 100039, People's Republic of China

G. Pan  
Lanzhou Institute of Chemical Industry, Research Institute  
of Lanzhou Petrochemical Company, PetroChina,  
Lanzhou 730000, People's Republic of China

found to have outstanding tribological properties. Therefore, they were generally used as solid lubricant to improve the tribological properties for the matrix [13–17]. Most of the researchers, have however, focused on the simulation of the tribological properties of graphene or on the study of the frictional properties of pristine graphene, whereas few studies have been devoted to the tribological behaviors of the GO/polymer nanocomposites [18–21].

As one of the most attractive matrixes in the polymer composites, nitrile rubber (NBR) has exhibited outstanding chemical resistance and a wide range of operating temperatures. Hence, NBR plays an outstanding role in the history of the development of elastomers for special applications [22–24]. Recent developments especially in the application of seal, automotive industries, and bearings required the development of NBR-based composites which exhibit low friction coefficient and excellent wear resistance under different lubrication conditions [25]. Thus, it is of interest and necessary to study the tribological properties of GO/NBR nanocomposites in both practical and scientific aspects.

In the current study, GO/NBR nanocomposites with various contents of GO were prepared and their tribological properties were investigated. The GO sheets were dispersed homogeneously in the NBR matrix using a simple solution-mixing method. The tribological properties of GO/NBR nanocomposites were measured by a ring-block wear tester under dry sliding and water-lubricating condition. In addition, the friction and wear mechanisms were tentatively proposed.

## Experiment

### Materials

Graphite flakes (325 mesh) were purchased from Qingdao Huatai Tech. Co., Ltd. NBR used in this study was N-41 (acrylonitrile content 29.6%, Mooney viscosity (ML (1 + 4)) at 100 °C: 78), which was gifted by Lanzhou chemical Industrial Co., Ltd of China. Carbon black (N220) was purchased from Tianjin Jinqiushi Chemical Co., Ltd. The chemicals included  $\text{KMnO}_4$ , concentrated  $\text{H}_2\text{SO}_4$ , HCl, and dimethyl formamide; all of which were of analytic grade. Other materials, such as Zinc Oxide, sulfur, stearic acid, etc., were commercial products.

### Preparation of graphene oxide

Graphene oxide (GO) was produced following an improved Hummers' method [26]. In brief, graphite flakes and  $\text{KMnO}_4$  were gradually added into the mixture of concentrated  $\text{H}_2\text{SO}_4/\text{H}_3\text{PO}_4$ , and then heated to 50 °C

followed by stirring 12 h. The mixture was cooled to room temperature and poured into cold (0 °C) deionized water. Then, 30%  $\text{H}_2\text{O}_2$  was added slowly into the mixture, until the solution turned into bright yellow. The resulting brilliant yellow mixture was centrifuged and washed with deionized water and 30% HCl for several times, until the pH of the mixture was neutral. Finally, the GO slurry was purified by dialysis for a week and then dried in a vacuum oven at 60 °C.

### Preparation of GO/NBR nanocomposites

The NBR was first cut into fragments and dissolved in a flask with 400 mL acetone at 60 °C by means of violent stirring. Simultaneously, the required amount of GO was dispersed in DMF by means of ultrasonication. Then, the GO/DMF suspension was gradually poured into the rubber solution and was stirred for 12 h. Finally, the deionized water was added to coagulate rubber and GO to produce the GO/NBR nanocomposites. Then, the nanocomposites were dried in a vacuum oven at 80 °C until its weight remained unchanged.

The nanocomposites were then mixed with the curing agents. The raw materials and formulation are summarized in Table 1. The blending process was carried out on a regular 6-inch two-roll mill (Lina Machine Industry Co., Ltd). Then, the samples were cured in a DY-100 plate vulcanizing press (Shanghai Dongye Electromechanical Machinery Co., Ltd) at 160 °C for 20 min under pressure of 10 MPa.

### Characterization and wear testing

#### Characterization

A JEM-2010 transmission electron microscopy (TEM) operating at an accelerating voltage of 200 kV was used to investigate the morphology of GO. Samples were first prepared by GO suspension in DMF. Then, the dispersion was dropped on a carbon-coated grid and dried in air for observation. The worn surfaces of the GO/NBR nanocomposites were investigated by scanning electron microscopy (JSM-5600LV, JEOL, Japan). Atomic force microscopy (AFM) images of GO were performed by a tapping mode by using a NanoscopeIIA instrument (AFM, Digital Instruments). The specimens were prepared by depositing GO suspension in DMF on a fresh silicon substrate and drying in air. The phase structure of the GO was measured by powder X-ray diffraction (XRD) apparatus on a Rigaku D/max-RB diffractometer with Ni-filtered graphite-monochromatized  $\text{Cu-K}\alpha$  radiation ( $\lambda = 1.54056 \text{ \AA}$ ). Fourier-transform infrared (FTIR) spectra were obtained using a Bruker IFS 66v/s IR Spectrophotometer over a frequency range of

**Table 1** Formulation of sulfur system for GO/NBR nanocomposite compounds

Materials	Amounts (phr <sup>a</sup> )
NBR	100
Carbon black (N220)	15
Sulfur	2
Zinc Oxide	5
Stearic acid	1.5
Accelerator CZ <sup>b</sup>	0.5
Accelerator TMTD <sup>c</sup>	0.25
GO	0, 0.5, 1.5, 3

<sup>a</sup> Parts per hundred parts in weight

<sup>b</sup> *N*-cyclohexyl-2-benzothiazolysulfenamide

<sup>c</sup> Tetramethylthiuram disulfide

400–4000 cm<sup>-1</sup>. The transfer film on the countersurface was investigated by optical microscopy (Olympus STM6).

### Wear testing

The friction and wear tests were performed on a ring-block (MRH-3, Jinan Yihua Tribology testing technology Co., Ltd) wear tester under dry sliding and water-lubricating condition. The wear test schematic diagram is shown in Fig. 1. A stainless steel ring was used as a counterpart with the outer diameter of 49.22 mm and the rubber blocks with the size of 12.32 × 12.32 × 19.05 mm. Before each test, the surface of counterpart was polished with metallographic abrasive paper. The test was conducted under ambient condition (temperature 20 ± 2 °C, humidity 30 ± 10%) and the sliding speed was 200 rpm under a normal load of 10 N for 1 h. At the end of each test, the width of wear scar was measured by the optical microscopy.

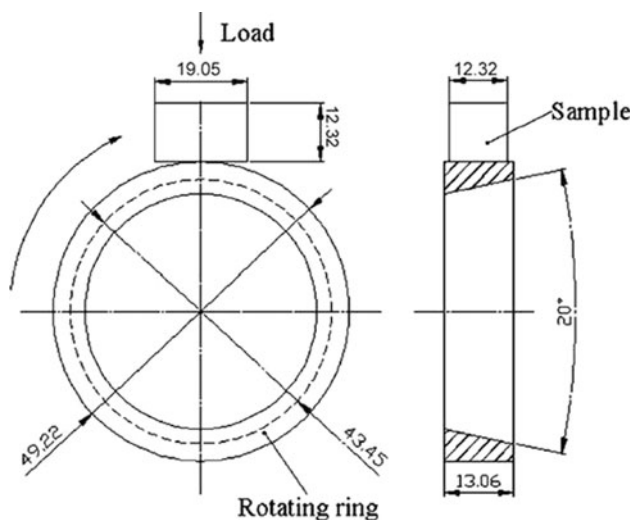


**Fig. 1** Schematic of sliding wear testing (unit: mm)

The specific wear rate ( $W_s$ ) was calculated using Eq. 1, and the volume of wear scar ( $V_s$ ) was obtained by Eq. 2.

$$W_s = V_s / F \cdot 2\pi R \cdot n \cdot t \quad (1)$$

$$V_s = \left[ \frac{\pi}{180} R^2 \arcsin \frac{b}{2R} - \frac{b}{2} \sqrt{R^2 - \frac{b^2}{4}} \right] B \quad (2)$$

where  $F$  is the normal load (N),  $R$  is the radius of steel ring (mm),  $b$  is the width of the wear scar (mm),  $B$  is the width of specimens (mm),  $n$  is the sliding speed (rpm), and  $t$  is the steady duration of friction (min).

## Results and discussion

### Characterization of GO and GO/NBR nanocomposites

The FTIR was carried out to study the functional groups of the GO. As shown in Fig. 2, the FTIR spectra of GO was recorded, and the following functional groups were existing in all the samples: the absorbance band at about 3417 cm<sup>-1</sup> could be attributed to the O–H-stretching vibration and the O–H stretching modes of intercalated water; C=O in carboxylic acid and carboxyl moieties ( $\nu$  (carboxyl)) at 1738 cm<sup>-1</sup>; C=C from unoxidized sp<sup>2</sup> cc bonds at ca. 1627 cm<sup>-1</sup>; C–O ( $\nu$  (epoxy or alkoxy)) at about 1076 cm<sup>-1</sup>. These results are consistent with the data reported in the literature [26–28].

AFM and TEM are currently the forefront methods allowing definitive identification of GO. As shown in Fig. 3a, the typical AFM image of GO revealed that the complete exfoliation of GO was achieved in DMF solution. The exfoliated GO sheet was approx 1.0 nm in thickness, 3.5 μm in length, and 2.1 μm in width. The GO had sheet morphology with some corrugation and scrolling because of the chemically modified GO sheets were decorated

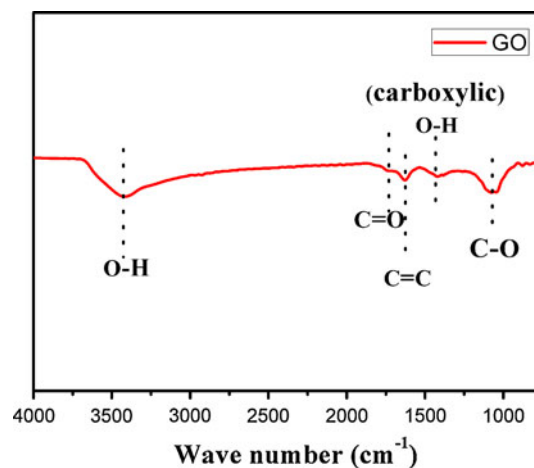


**Fig. 2** FTIR spectrums of GO

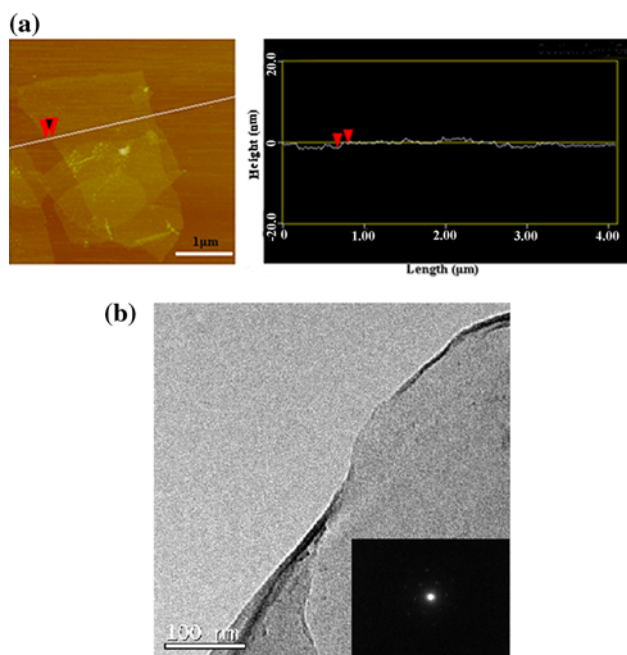


**Fig. 3** **a** Tapping mode AFM topographic image and height profiles of GO and **b** TEM Images of layered GO

mostly with oxygen-containing functional groups, which prevented the GO sheets from stacking back and regraphitization. TEM was conducted to further characterize the exact structures of GO in the dispersions. As shown in Fig. 3b, a large and transparent GO sheet was clearly observed, and the sheet edges scrolled and folded slightly. It is well known that the corrugation and scrolling are a part of the intrinsic nature of graphene sheets, which result from because 2D membrane structure becomes thermodynamically stable via bending [29, 30]. The inset depicts the electron diffraction pattern of the GO sheet, and the diffraction rings and dots revealed ordered graphitic lattices.

As the FTIR spectra show, there is a plenty of oxygen-containing functional groups on the surfaces of the chemical-modified GO sheets, such as epoxide and hydroxyl groups, in addition to carbonyl and carboxyl groups. These oxygen functionalities will alter the Van Der Walls interactions between the layers and make them hydrophilic. Therefore, the GO sheets could readily exfoliate in DMF and form a stable solution with GO concentration of 0.2 mg/mL, as shown in Fig. 4a. The solution was well mixed with NBR/acetone solution and yielded a homogeneous mixture as shown in Fig. 4b. After vulcanization process, the dispersion of GO sheets in NBR matrix was observed by SEM. As shown in Fig. 4c, one could find that no obvious GO aggregates were observed from the cross sections of the nanocomposites, which revealed that the GO sheets were homogeneously dispersed in NBR matrix. As shown in Fig. 4d, the arrows point that there there some

wrinkled GO sheets that are pulled out of NBR matrix, because the surface-coatings caused by NBR on the GO sheets in NBR matrix are much thicker than those on the original GO sheets [12].

The dispersion of GO in the NBR matrix was further confirmed by XRD. As shown in Fig. 5, the diffraction peak of GO (curve a) appears at  $2\theta = 11.7^\circ$  (the  $d$ -spacing is 0.75 nm), which is the typical peak of the layered GO. It indicated that the graphite had been successfully exfoliated during the chemical-modification process [31]. It is seen from the curve b that a broad diffraction peak of NBR appears, indicating the noncrystalline structure of the vulcanized NBR. The GO/NBR nanocomposite with 0.5 wt% GO (curve c) has only a broad diffraction from  $15^\circ$  to  $30^\circ$ , which demonstrates that the ordered structure of the layered GO have been destroyed during the compounding process [32–34]. For the GO/NBR nanocomposites with different GO contents (curves d, and e), similar results are obtained. The findings described above indicate that the layered GO/NBR nanocomposites have been successfully prepared.

#### Tribological behaviors under dry sliding condition

The friction coefficient (COF) and specific wear rate of GO/NBR nanocomposites, with different contents of GO are shown in Fig. 6. It indicated that under dry sliding condition both the COF and specific wear rate of GO/NBR nanocomposites decreased dramatically at first, then increased with the increasing GO content. When the GO was incorporated, the COF and specific wear rate of GO/NBR nanocomposites could be effectively reduced because the fundamental graphite lattices of GO consisted of loosely bound layers which intrinsically possess low shear strength [18]. It could be seen that the COF and specific wear rate of GO/NBR nanocomposites reached the lowest values when the GO content was 0.5 wt%. This may be due to the homogenous dispersion of GO and the excellent tribological properties of multilayered GO [19]. It also demonstrated that higher GO contents seemed to lead to the degradation of wear resistance and the increase of COF. When sliding on the steel counterface under dry sliding, the formation of the transfer film was always thought to be an important factor to enhance the wear resistance of the polymer composite [35–38]. In this article, the transfer films were investigated by optical microscopy (Olympus STM6). As shown in Fig. 7a, a lot of black dots and notch were found on the countersurface for the NBR without GO. It indicated that continuous transfer film could not form for the composites without GO under dry sliding condition. Therefore, the vulcanized NBR exhibited a high COF and a weak wear resistance. In Fig. 7b, for the GO/NBR nanocomposites with the content of GO of 0.5 wt%, the surface of the counterpart became smoother and the black dot

**Fig. 4** Photograph of GO dispersion in DMF (a) and GO/NBR nanocomposites in DMF (b); SEM image of GO/NBR nanocomposites with GO concentration of 3 wt% (c) and (d)

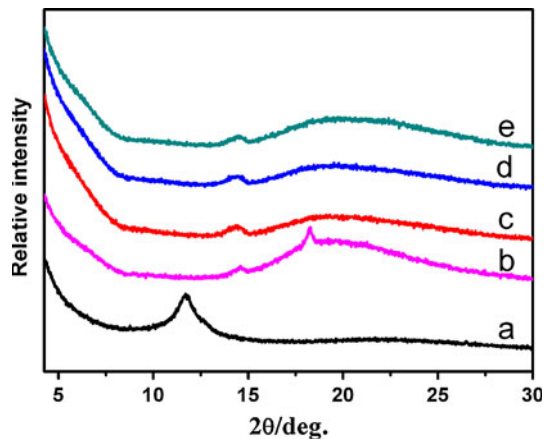
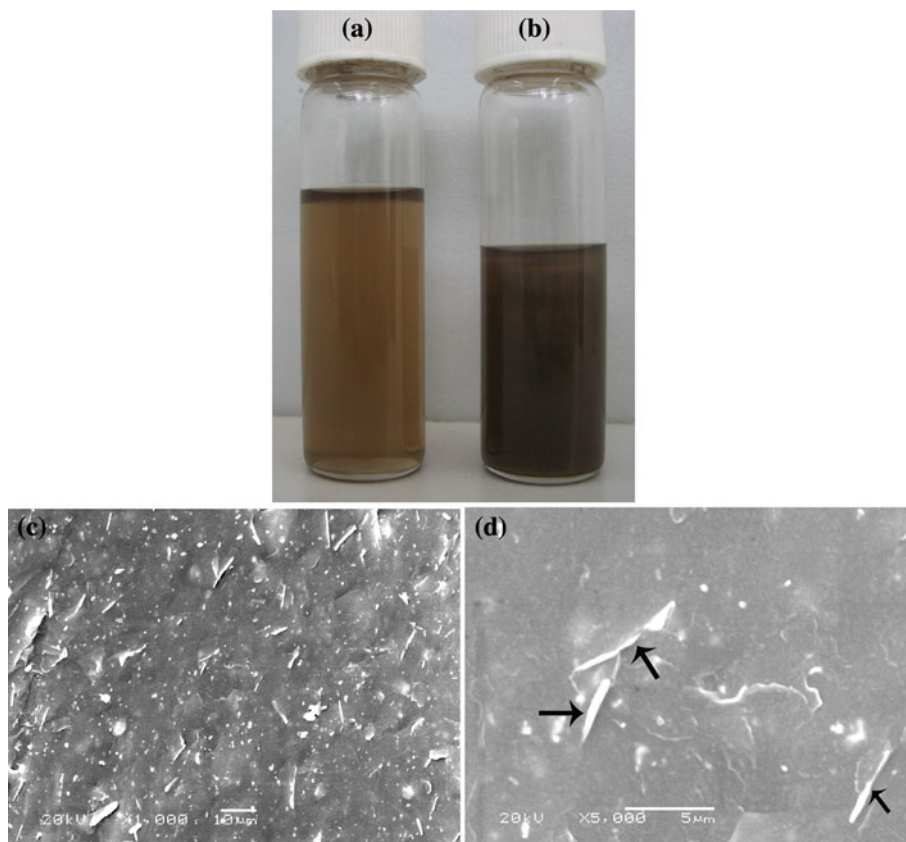


**Fig. 5** XRD patterns of a GO; b NBR; c 0.5 wt%; d 1.5 wt%; e 3 wt% GO/NBR composites

disappeared, which indicated that a continuous and compact transfer film was formed on the surface of counterpart. A continuous and compact transfer film could dramatically reduce the COF and increase the wear resistance of nanocomposite [39–41]. As shown in Fig. 7c, when the content of GO was 1.5 wt%, the transfer film became loose which corresponded to the higher COF of the GO/NBR nanocomposites (Fig. 5). When the GO weight content was further increased to 3 wt%, the continuous and compact

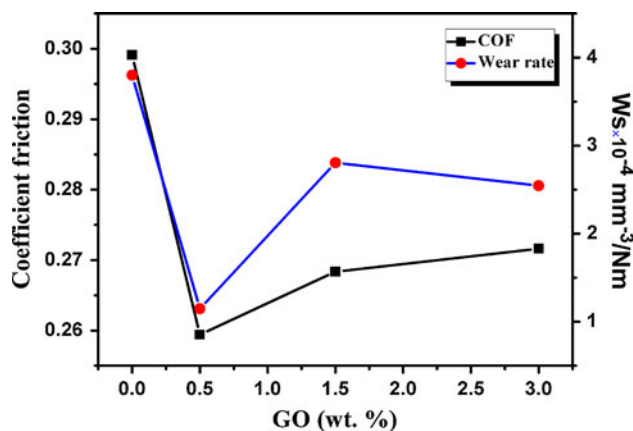


**Fig. 6** Variation for the COF and the specific wear rate of GO/NBR nanocomposites with different content of GO under dry sliding condition

transfer film was destroyed, and many black dots are found again in Fig. 7d. The results showed that the higher content of GO led to a weak wear resistance.

In order to identify the types and intensity of friction and wear of the GO/NBR nanocomposites, the center of wear scars for all the specimens were investigated by SEM. As shown in Fig. 8a, a large number of debris and deep plow grooves were found on the worn surface of vulcanized

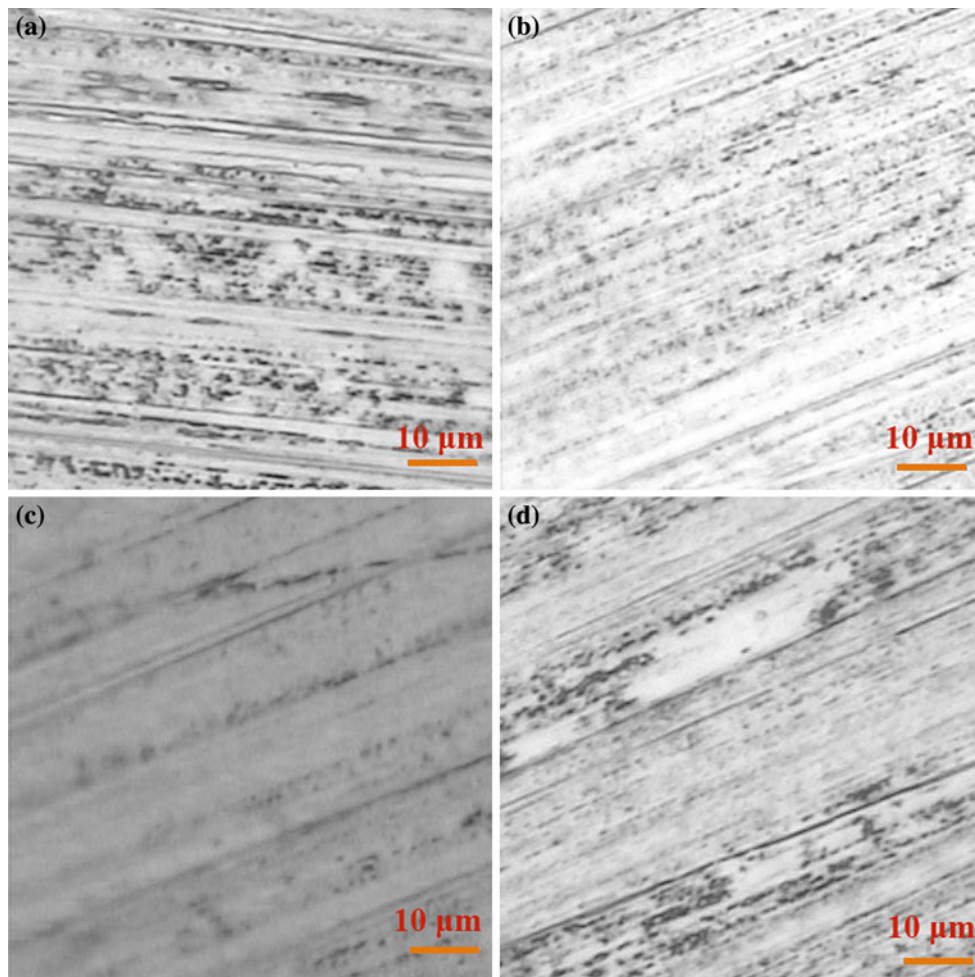


**Fig. 7** Photographs of transfer film on countersurfaces: **a** NBR; **b** 0.5 wt%; **c** 1.5 wt%; **d** 3 wt% GO/NBR nanocomposites under dry sliding condition

NBR without GO, which indicated that the vulcanized NBR exhibited extremely abrasive wear under dry sliding. This result corresponded to the high COF of the vulcanized NBR without GO (Fig. 6). As shown in Fig. 8b, when the GO content reached 0.5 wt%, the huge plow grooves became narrower, and the worn surface became smoother. It indicated that a transfer film was formed on the countersurface. In Fig. 8c, the worn surface of specimen with GO (1.5 wt%) showed adhesive spalling, but much of the area of the worn surface was integrated. It is concluded that the wear mechanism gradually changed from that of abrasive grain and adhesion abrasion mainly to that of adhesion and fatigue abrasion, largely because of increasing GO content. In Fig. 8d, the specimen with GO content of 3 wt% showed obvious adhesive spalling, and a large area of the worn surface was spalled.

According to the analysis of the tribological behaviors of GO/NBR nanocomposites under dry sliding condition, it

could be hypothesized that the wear mechanism changed with the variation of GO content. The GO would be spalled and transferred from the matrix to the surface of counterpart in the friction process. Then, the spalling GO filled the notch of the counterpart surface and formed a dynamic transfer film. Similar results have been observed for graphite/epoxy two-phase composite coatings [14]. The schematic diagram of dynamic process is shown in Fig. 9, which exhibits the formation of transfer film and the spalling of abrasive debris. The thickness of the transfer film increased with the increasing GO contents. When the transfer film was formed, it could effectively reduce the direct contact area of metal slider and rubber block, and cause the friction process between the transfer film and the lubricated rubber surface. Therefore, the COF and specific wear rate of GO/NBR nanocomposites could be drastically decreased. However, as the weight content of GO was higher than 0.5 wt%, it would lead to the breaking of

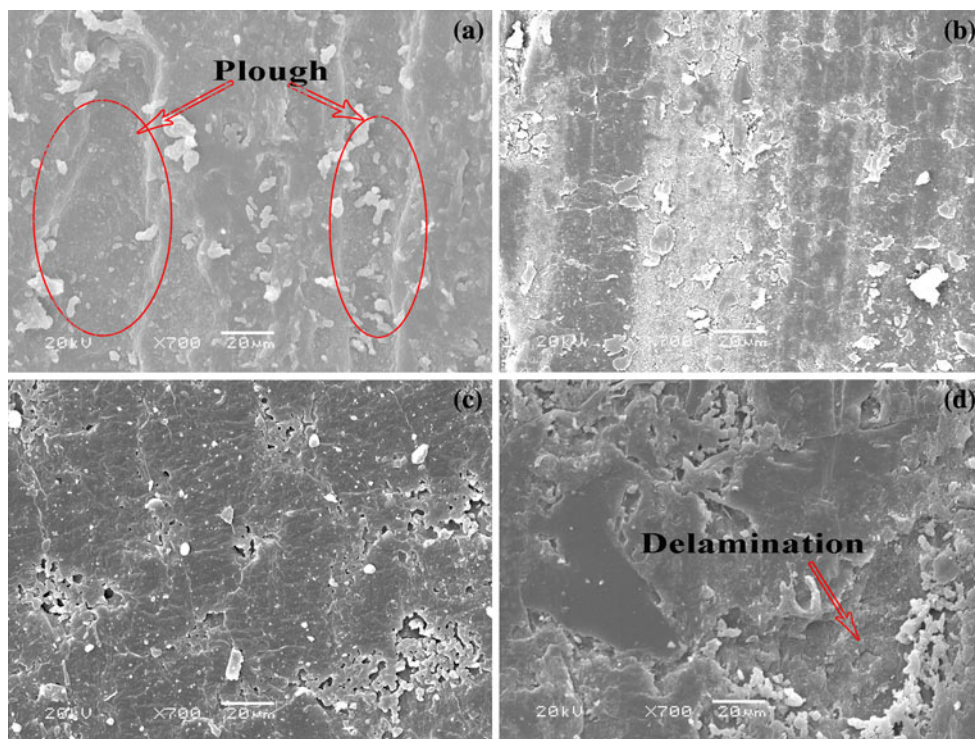


**Fig. 8** SEM images of worn surface of the specimens: **a** NBR; **b** 0.5 wt%; **c** 1.5 wt%; **d** 3 wt% GO/NBR nanocomposites under dry sliding condition

dynamic equilibrium and speeding up the spalling of transfer film and debris. Therefore, wear mechanism changed from abrasive grain and adhesion abrasion to adhesion and fatigue abrasion because of the increasing GO content.

#### Tribological behaviors under water-lubricating condition

As shown in Fig. 10, under water-lubricated condition, the COF and specific wear rate of the NBR and GO/NBR nanocomposites were obviously lower than that obtained from dry sliding tests. Both the COF and specific wear rate of the GO/NBR nanocomposites decreased with increasing GO content. Because NBR matrix contained CN polar group and the GO had hydrophilic groups, the surfaces of specimens could form strong hydrogen bonding with the water molecules, leading to the formation of continuous water film between the rubber block and countersurface, which could drastically reduce the COF and specific wear rate of the specimens. The reasons that the water film could drastically improve the tribological properties of the nanocomposites were proposed as follows [42–44]:

- (1) The water-lubricated film could reduce the direct contact area of metal slider and rubber block.
- (2) The debris was taken away by water so that it could effectively reduce the abrasive wear.

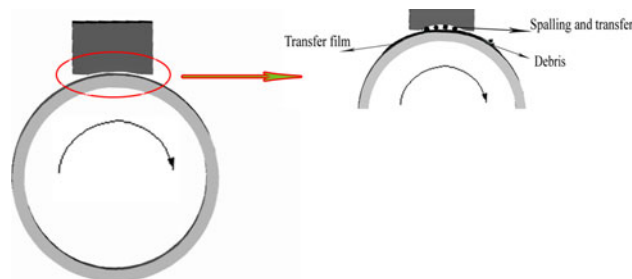


**Fig. 9** Schematic of spalling and transfer of GO between the friction couple during dry sliding wear testing

- (3) It is well known that when two bodies are rubbed together heat is produced, thus raising both their the surface temperatures. Under water-lubricating condition, the friction heat was effectively reduced, and this lightened the adhesive wear.

To identify the effect of GO on the wear resistance of the nanocomposites under water-lubricating condition, the worn surface of the specimens were observed by the SEM. The morphologies of the worn surfaces are shown in Fig. 11. Compared with Fig. 8, it could be found that the surfaces of NBR and NBR/GO nanocomposites were worn more severely under dry sliding than the under water-lubricated condition. Furthermore, the worn surface under water lubricated condition displayed less plow and

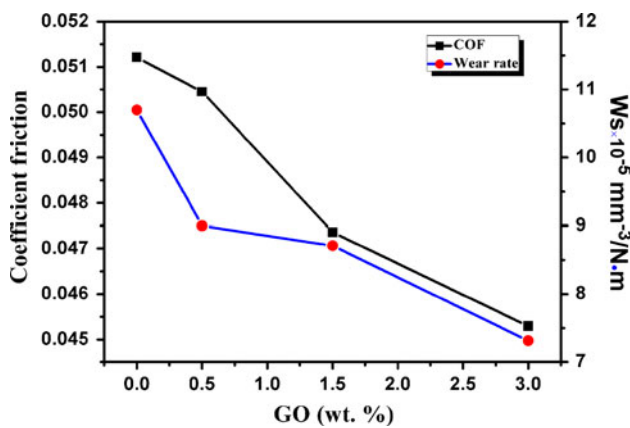


**Fig. 10** Variation for the COF and the specific wear rate of GO/NBR nanocomposites with different content of GO under water lubricating condition

delamination. It revealed that under water-lubricated condition, water was not only a kind of polar lubricant for specimens to reduce the direct contact zone of rubber blocks with stainless steel counterfaces, but it also dissipated the frictional heat during the sliding. Thus, the COFs of NBR and its nanocomposites were lower in water than those in dry sliding. As well, it revealed that the specimens were dominated by adhesion wear under water-lubricated condition. Among the tested materials, GO/NBR nanocomposites displayed a higher wear resistance than that of

NBR. The worn surfaces of specimens became smoother with increasing GO contents. This could be attributed to the hydrophilic groups of GO, which could form strong hydrogen bonding with the water molecules, leading to the formation of a thicker water film between the rubber block and countersurface under water-lubricated condition.

**Conclusion**

A series of NBR/GO nanocomposites were prepared by a solution-mixing method. The tribological properties of GO/NBR under dry sliding and water-lubricated condition have been investigated. Also, the effects of GO on the wear behavior have been discussed. The results discussed in this study could potentially aid in rational design and the use of self-lubricating composites and the most important conclusions as follows could be drawn:

1. Exfoliated GO sheets were successfully prepared by an improved Hummers’ method, and the GO sheets were dispersed homogeneously in the NBR matrix by a simple solution-mixing method.
2. Under dry sliding, the GO could easily transfer from the matrix to the counterpart surface to form a continuous and compact transfer film. Thereby, the composites displayed excellent friction reduction and

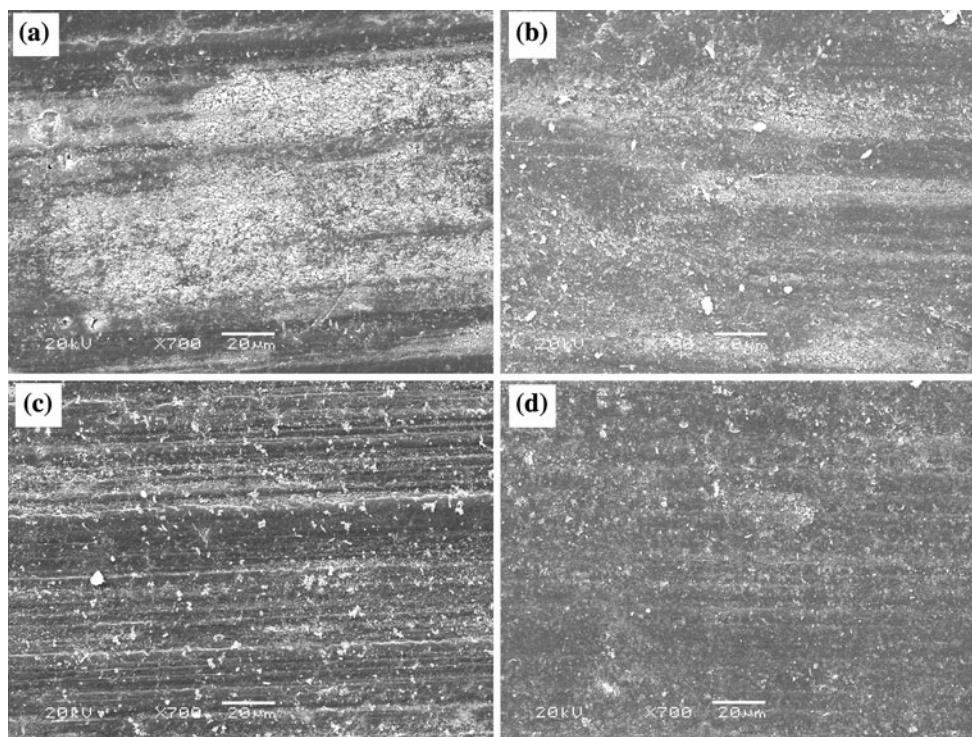


**Fig. 11** SEM images of worn surface of the specimens: **a** NBR; **b** 0.5 wt%; **c** 1.5 wt%; **d** 3 wt% GO/NBR nanocomposites under water lubricating condition



wear resistance properties at a low GO loading. When GO content is higher than 0.5 wt%, the COF and specific wear rate of the composites increased with increasing GO content.

- Under water-lubricating condition, both the COF and specific wear rate of nanocomposites were decreased with increasing GO contents. It could be attributed to the hydrophilic groups of GO, which could form strong hydrogen bonding with the water molecules, leading to the formation of a thicker water film between the rubber block and countersurface.

**Acknowledgements** The authors would like to acknowledge the financial supports from the National Science Foundation for Distinguished Young Scholars of China (Grant No. 51025517), the Innovative Group Foundation of NSFC (Grant No. 50721062), and the 973 Project of China (2007CB607606), the National Defense Basic Scientific Research Project (A1320110011).

## References

- Geim AK (2009) *Science* 324(5934):1530. doi:10.1126/science.1158877
- Verdejo R, Bernal MM, Romasanta LJ, Lopez-Manchado MA (2011) *J Mater Chem* 21:3301
- Jang BZ, Zhamu A (2008) *J Mater Sci* 43(15):5092. doi:10.1007/s10853-008-2755-2
- Tibbetts GG, Lake ML, Strong KL, Rice BP (2007) *Compos Sci Technol* 67(7–8):1709. doi:10.1016/j.compscitech.2006.06.015
- Wang Y, Shi ZX, Fang JH, Xu HJ, Yin J (2011) *Carbon* 49(4):1199. doi:10.1016/j.carbon.2010.11.036
- Kim H, Macosko CW (2009) *Polymer* 50(15):3797. doi:10.1016/j.polymer.2009.05.038
- Ajayan PM, Schadler LS, Giannaris C, Rubio A (2000) *Adv Mater* 12(10):750
- Qiu JJ, Wang SR (2011) *J Appl Polym Sci* 119(6):3670. doi:10.1002/app.33068
- Pan YZ, Wu TF, Bao HQ, Li L (2011) *Carbohydr Polym* 83(4):1908. doi:10.1016/j.carbpol.2010.10.054
- Li R, Liu CH, Ma J (2011) *Carbohydr Polym* 84(1):631. doi:10.1016/j.carbpol.2010.12.041
- Jung JH, Jeon JH, Sridhar V, Oh IK (2011) *Carbon* 49(4):1279. doi:10.1016/j.carbon.2010.11.047
- Bai X, Wan CY, Zhang Y, Zhai YH (2011) *Carbon* 49(5):1608. doi:10.1016/j.carbon.2010.12.043
- Saffar A, Shojaei A, Arjmand M (2010) *Wear* 269(1–2):145. doi:10.1016/j.wear.2010.03.021
- Pan GL, Guo QA, Ding JA, Zhang WD, Wang XM (2010) *Tribol Int* 43(8):1318. doi:10.1016/j.triboint.2009.12.068
- Österle W, Dörfel I, Prietzel C, Rooch H, Cristol-Bulthé AL, Degallaix G, Desplanques Y (2009) *Wear* 267(5–8):781. doi:10.1016/j.wear.2008.11.023
- Yu S, Hu H, Yin J (2008) *Wear* 265(3–4):361. doi:10.1016/j.wear.2007.11.006
- Schön J (2000) *Wear* 237(1):77. doi:10.1016/s0043-1648(99)00315-4
- Lee H, Lee N, Seo Y, Eom J, Lee S (2009) *Nanotechnology* 20(32). doi:10.1088/0957-4484/20/32/325701
- Lee C, Li QY, Kalb W, Liu XZ, Berger H, Carpick RW, Hone J (2010) *Science* 328(5974):76. doi:10.1126/science.1184167
- Lee C, Wei X, Li Q, Carpick R, Kysar JW, Hone J (2009) *Phys Stat Sol b* 246(11–12):2562. doi:10.1002/pssb.200982329
- Bonelli F, Manini N, Cadelano E, Colombo L (2009) *Eur Phys J B* 70(4):449. doi:10.1140/epjb/e2009-00239-7
- Kaiser A, Brandau S, Klimpel M, Barner-Kowollik C (2010) *Macromol Rapid Commun* 31(18):1616. doi:10.1002/marc.201000162
- Kader MA, Kim K, Lee YS, Nah C (2006) *J Mater Sci* 41(22):7341. doi:10.1007/s10853-006-0792-2
- Hsieh TH, Kinloch AJ, Masania K, Lee JS, Taylor AC, Sprenger S (2010) *J Mater Sci* 45(5):1193. doi:10.1007/s10853-009-4064-9
- Degrange JM, Thomine A, Kapsa P, Pelletier JM, Chazeau L, Vigier G, Dudragne G, Guerbe L (2005) *Wear* 259(1–6):684. doi:10.1016/j.wear.2005.02.110
- Marcano DC, Kosynkin DV, Berlin JM, Sinitskii A, Sun ZZ, Slesarev A, Alemany LB, Lu W, Tour JM (2010) *ACS Nano* 4(8):4806. doi:10.1021/nn1006368
- Guo HL, Wang XF, Qian QY, Wang FB, Xia XH (2009) *ACS Nano* 3(9):2653. doi:10.1021/nn900227d
- Rourke JP, Pandey PA, Moore JJ, Bates M, Kinloch IA, Young RJ, Wilson NR (2011) *Angew Chem Int Ed* 50(14):3173. doi:10.1002/anie.201007520
- Shen JF, Hu YZ, Shi M, Lu X, Qin C, Li C, Ye MX (2009) *Chem Mater* 21(15):3514. doi:10.1021/cm901247t
- Wilson NR, Pandey PA, Beanland R, Young RJ, Kinloch IA, Gong L, Liu Z, Suenaga K, Rourke JP, York SJ, Sloan J (2009) *ACS Nano* 3(9):2547. doi:10.1021/nn900694t
- Park S, Ruoff RS (2009) *Nat Nano* 4(4):217
- Das A, Jurk R, Stockelhuber KW, Heinrich G (2007) *Exp Polym Lett* 1(11):717. doi:10.3144/expresspolymlett.2007.99
- Bai X, Wan C, Zhang Y, Zhai Y (2011) *Carbon* 49(5):1608. doi:10.1016/j.carbon.2010.12.043
- Xu J, Hu Y, Song L, Wang Q, Fan W, Chen Z (2002) *Carbon* 40(3):450. doi:10.1016/s0008-6223(01)00134-8
- Gu F, Zhang ZZ, Liu WM, Su FH, Zhang HJ (2008) *J Appl Polym Sci* 110(3):1771. doi:10.1002/app.28124
- Lai SQ, Li TS, Liu XJ, Lv RG (2004) *Macromol Mater Eng* 289(10):916. doi:10.1002/mame.200400140
- Buckley DH, Brainard WA (1975) *Carbon* 13(6):501. doi:10.1016/0008-6223(75)90052-4
- Xu D, Karger-Kocsis J (2010) *J Mater Sci* 45(5):1293. doi:10.1007/s10853-009-4081-8
- Kaneko D, Oshikawa M, Yamaguchi T, Gong JP, Doi M (2007) *J Phys Soc Jpn* 76 (4). doi:10.1143/jpsj.76.043601
- Bahadur S (2000) *Wear* 245(1–2):92. doi:10.1016/s0043-1648(00)00469-5
- Ziemianski K, Pietrasik R (1979) *Wear* 56(1):123. doi:10.1016/0043-1648(79)90011-5
- Srinath G, Gnanamoorthy R (2007) *Compos Sci Technol* 67(3–4):399. doi:10.1016/j.compscitech.2006.09.004
- Jia JH, Chen JM, Zhou HD, Wang JB, Zhou H (2004) *Tribol Int* 37(5):423. doi:10.1016/j.triboint.2003.12.013
- Meng H, Sui GX, Xie GY, Yang R (2009) *Compos Sci Technol* 69(5):606. doi:10.1016/j.compscitech.2008.12.004